BREACH WIDENING OBSERVATIONS FROM EARTHEN EMBANKMENT TESTS

S. L. Hunt, G. J. Hanson, K. R. Cook, K. C. Kadavy

ABSTRACT. *In recent years, interest has risen in the occurrence and effects of overtopping on earth embankments due to the number of dams that have reached the end of their planned service life. The embankment failure process due to overtopping includes several aspects of erosion: failure of the vegetation, concentrated flow, headcut migration, and breach timing, formation, and widening. Research using large-scale physical models is on-going at the USDA-ARS Hydraulic Engineering Unit to provide a better understanding of how a breach develops over time and what variables influence breach development. Soil properties have been observed to greatly influence how a soil erodes and therefore influence the embankment erosion processes, including breach widening. The objective of this article is to evaluate the time rate of breach widening of three large-scale earthen embankment tests. The embankments were constructed of homogeneous materials ranging from silty sand to lean clay, 1.3 m in height with a 0.30 m notch through the center of the embankment. The primary erosion process of interest during these tests was breach widening. The results from these tests as well as widening data from previous embankment overtopping tests conducted at the laboratory are compared in relation to the compaction water content of the soils used to construct the embankments. Rates of widening were strongly influenced by the compaction water content. Measured soil properties are promising in characterizing the development of a breach.*

Keywords. *Breach, Dams, Embankments, Erodibility, Erosion, Flooding, Headcut, Overtopping, Soil parameters.*

As a result of Congressional passage of the Flood Control Act of 1944 and the Watershed Protection and Flood Control Act of 1953, the USDA Natural Resources Conservation Service (NRCS) has helped design and construct over 11,000 small watershed dams (USDA-NRCS, 2005). Upon evaluation of the USDA-NRCS flood retarding structures, it is currently estimated that more than half of the 11,000 NRCS dams are more than 30 years old, and by the end of 2008, over 1000 of these watershed dams will reach the end of their planned service life (USDA-NRCS, 2005). One of the issues related to rehabilitation of these structures is dam safety, including dam failure due to embankment overtopping. Overtopping generally occurs when the inflow into the reservoir exceeds the auxiliary spillway capacity and the storage capacity of the reservoir. Although the risk to embankment overtopping failure can be reduced by increasing the storage capacity of the reservoir (i.e., raising the top of dam and/or auxiliary spillway crest) or widening the auxiliary spillway to increase flow capacity, allowable overtopping is one alternative that is being considered for rehabilitation. However, to seriously consider this alternative, predicting embankment performance and failure is crucial.

Embankment overtopping failure is a function of the erosion processes and erosion rates that occur during overtopping. Ralston (1987), in his discussion of dam overtopping and failure, distinguished between non-cohesive and cohesive soil embankments and the failure processes. Ralston described the erosion process for non-cohesive embankments as a sediment transport process involving material removal from the embankment in layers and for cohesive embankments as involving the formation and migration of a headcut through the embankment. Ralston also observed that most dams that are medium to small in height are built of cohesive soil materials and that most large dams have a cohesive inner core, therefore pointing out the importance of understanding the failure processes of cohesive embankments.

Hanson et al. (2003a), based on observations from seven large-scale embankment overtopping failure tests, described a four-stage erosion process for cohesive embankments (fig. 1). Stage I begins when the initial flow overtops the embankment, resulting in sheet and rill erosion on the downstream face of the embankment and then developing into a series of cascading overfalls. This stage ends when the cascading overfalls develop into one large headcut that migrates through the downstream embankment face to the downstream crest such that the width of erosion is approximately equal to the width of the flow at the downstream crest. Stage II occurs as the headcut migrates from the downstream embankment crest to the upstream embankment crest. Stage III occurs as the embankment crest lowers, ending as the downward erosion of the crest has virtually stopped. Stage IV begins after the breach opening has eroded to near the base of the upstream toe of the embankment and is the

Article was submitted for review in January 2004; approved for publication by the Soil & Water Division of ASAE in April 2005. Presented at the 2004 ASAE Annual Meeting as Paper No. 042080.

The authors are **Sherry L. Hunt, ASAE Member Engineer,** Research Hydraulic Engineer, and **Gregory J. Hanson, ASAE Member Engineer,** Research Hydraulic Engineer, USDA-ARS, Stillwater, Oklahoma; **Kevin R. Cook, ASAE Member Engineer,** Geotechnical Engineer, USDA-NRCS, Stillwater, Oklahoma; and **Kem C. Kadavy, ASAE Member Engineer,** Agricultural Engineer, USDA-ARS, Stillwater, Oklahoma. **Corresponding author:** Sherry Hunt, USDA-ARS, 1301 N. Western, Stillwater, OK 74075; phone: 405-624-4135, ext. 222; fax: 405-624-4136; e-mail: sherry.hunt@ars.usda.gov.

Figure 1. Erosion processes during overtopping test: (a) rills and cascade of small overfalls during stage I, (b) consolidation of small overfalls during stage I, (c) headcut at downstream crest, transition from stage I to stage II, (d) headcut at upstream crest, transition from stage II to stage III, (e) flow through breach during stage III, and (f) transition from stage III to stage IV (Hanson et al., 2003a).

stage at which the breach widens as flow is released from the reservoir following breach formation. Widening occurs during all stages of the erosion process; during stage IV, the breach process influences reservoir discharge.

Researchers including Coleman et al. (2002), Visser (1998), Pugh (1985), and Tinney and Hsu (1961) have investigated the widening processes once a breach has fully formed, but these investigations focused on non-cohesive embankments or fuse plugs. Coleman et al. (2002) presented overtopping breach results of small-scale tests on non-cohesive embankments, which included breach widening observations. They observed that their results were not a function of the embankment materials and therefore developed a lateral widening relationship that was strictly a function of time. Visser (1998) developed widening algorithms for breach growth of sand dikes based on sediment transport algorithms. Pugh (1985) conducted fuse plug tests and concluded that even though the fuse plugs had a clay core, the geometry of the core was such that the rate of widening could be determined based on an empirical relationship. This was because the erosion of the non-cohesive embankment material downstream of the core controlled the widening. These types of approaches, even though apparently adequate for non-cohesive embankments, dikes, and fuse plugs, are arguably not appropriate for cohesive embankments in which rates of erosion are strongly influenced by soil material properties, including water content, density, erodibility, strength, and compaction (Hanson et al., 2003b).

The processes and rates of the first three stages of breach formation of cohesive embankments are described by Hanson et al. (2003a, 2003b). The focus of this article is on stage IV, the breach widening processes and determination of the rate of widening. Stage IV widening is of key importance in predicting the rate of water released from reservoirs that still contain large volumes of water following the first three stages of the embankment breach process. Large volumes of water will remain following the first three stages of breach formation for reservoirs with large storage capacity relative to the breach formation rate. This article summarizes the observed breach widening for three large-scale cohesive embankment tests simulating stage IV conditions and

Table 1. Soil properties.

Embankment	Soil	Sand >75 μm[a] (%)	Fines >2 μm[a] (%)	Fines <2 μm[a] (%)	PI[b]	Soil Classification[a]	WC[c] (%)	γ_d[d] (kN m^{-3})
W1	2	63	31	6	NP	SM - silty sand	12.2	17.6
W2	2	63	31	6	NP	SM - silty sand	10.7	17.6
W3	3	25	49	26	17	CL - lean clay	16.2	16.7

ASTM Standards used to measure soil properties: [a]D 2487, [b]D 4318, [c]D 4959, and [d]D 2937.

compares the widening results with widening observations for stages II and III reported by Hanson et al (2003a, 2003b). These results will be important in the development and validation of computer models for breach simulations.

Experimental Setup and Methods

Three large-scale earthen embankments were constructed at the USDA-ARS Hydraulic Engineering Unit in Stillwater, Oklahoma, to evaluate the widening of a breach over time. The embankments were constructed of cohesive homogeneous materials ranging from a silty sand to a lean clay. The embankments were constructed in lifts, with a compacted lift thickness of 0.09 m. The soils were compacted using a self-propelled vibratory pad-foot roller. Each lift was compacted with two passes of the roller in vibration mode. Tube samples were taken from each compacted lift to determine the compaction density and compaction water content. Particle size distribution, plasticity index (PI), and soil classification were determined from disturbed samples taken from previous embankment tests. These tests were conducted at the USDA-NRCS National Soil Testing Lab (NSTL) in Fort Worth, Texas (table 1).

The constructed embankments were 1.3 m in height with a 1.8 m crest width and 3:1 (H:V) side slopes on the upstream and downstream faces (fig. 2). The width of the test section was 5.5 m. Just prior to testing, a 0.30 m wide notch was cut through the center of the entire height of the embankment with a backhoe. The notch was then backfilled with sand prior to testing to protect the notch opening as the reservoir filled.

Chart recorders fitted with digital encoders were utilized to record the inflow and outflow hydrographs during testing. An overhead rolling carriage with an attached point gauge was utilized to obtain bed profiles, cross sections, and water surface elevations during testing (fig. 3). A digital camera was placed in a fixed location for photographic documentation of breach width (fig. 4). Inflow to the reservoir during testing was supplied by canal and measured at the test site with a sharp-crested weir. On the day of testing, the reservoir was completely filled, and the embankment test notch overtopped. The sand in the pre-cut notch quickly eroded away, and breach widening began. The inflow discharge stabilized quickly during tests W1 and W2 at a relatively constant flow of about 2.9 m^3 s^{-1} for each embankment, while the inflow discharge during the majority of test W3 was maintained at 1.36 m^3 s^{-1} (fig. 5a). The test setup allowed flow to either pass through the breach in the embankment or over a 43 m long weir, located upstream of the test embankment. The purpose of this setup was to maintain a relatively constant pool elevation upstream of the breach opening (fig. 5b). As the breach widened, less water passed over the weir and more passed through the breach. At some point during the testing of the embankments, the flow passed entirely through the breach and no longer over the weir. A

Figure 2. Embankment widening test.

Figure 3. Point gauge carriage for measuring water surface and bed surface elevations.

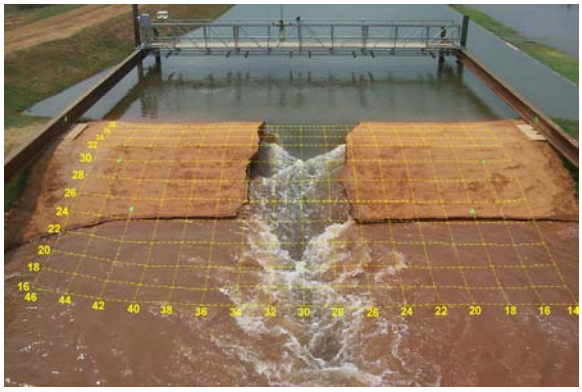

Figure 4. Photographic measurements of erosion width.

chart recorder fitted with a digital encoder was used to track reservoir elevation, and a manually read staff gauge was used for tailwater measurements. Reservoir elevation was used to determine the volume of storage in the reservoir at any given time during the test and to determine the discharge over the weir. The outflow hydrograph through the notch opening for

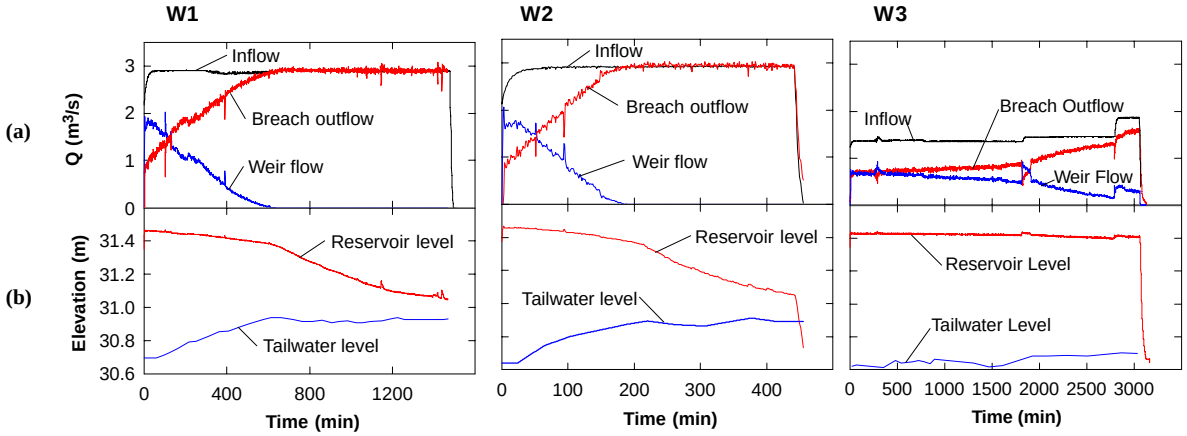

Figure 5. Tests W1, W2, and W3: (a) inflow breach and weir flows, and (b) reservoir and tailwater levels.

each of the tests was determined based on inflow, change in storage, and flow over the weir.

Observations and Discussion

The three embankment widening tests discussed herein are comparable to stage IV of the erosion process as described by Hanson et al. (2003a). Stage IV begins after the breach opening has eroded to near the base of the upstream toe of the embankment and is the stage at which the breach widens as flow is released from the reservoir following breach formation.

Similar to that described by Coleman et al. (1997), the breach channel widened in all three tests to a large extent as the channel sides became undermined, causing mass failures to occur. The undermining was observed to occur as a detachment process, resulting in an overhang developing. A crack along the surface was observed at the initiation of mass failure of the bank (fig. 6). The crack slowly opened, and eventually the material toppled into the breach opening. Since breach widening was the primary focus of tests W1, W2, and W3, one of the more important measurements was breach width. This was accomplished in two ways: (1) profile measurements at periodic times during the flow (fig. 3), and (2) taking measurements from digital imagery (fig. 4). The initial notch width was 0.30 m and widened as mass failures occurred. Therefore, the widening occurred in episodic fashion as each bank failed during the duration of the test. Figure 7 shows the episodic widening that occurred at the downstream crest (station 32) for test W2. The episodic width increase at the time of each mass failure for the three tests varied from 0.2 to 1 m with an average of 0.6 m. The average of 0.6 m is approximately half of the embankment height, which was 1.2 m for the three tests. This is consistent with observations made by Terzaghi (1941) in that tension cracks tended to form at a distance of half the vertical bank height back from the bank edge.

The rate of breach widening (dW/dt) was determined by taking the linear regression of the breach width measurement from left bank to right bankversus time during the period that the flow was both going over the upstream weir and through the breach (fig. 8). During this period of time, the reservoir water level was maintained at a relatively constant level and the hydraulic stresses on the breach sidewalls could be assumed to be constant. Since the reservoir water level was

Figure 6. Formation of a crack prior to mass failure.

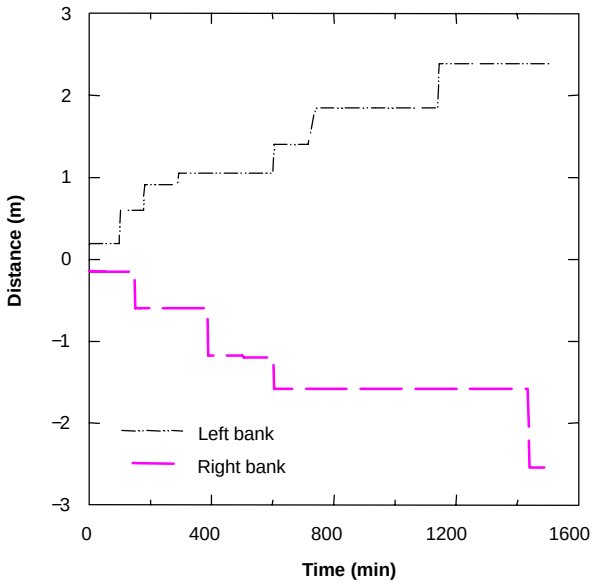

Figure 7. Episodic breach widening measurements from left and right banks.

the same during this time in all three tests, the hydraulic stress could be assumed to be the same between tests as well. The breach widening rates during these periods of time were determined to be 0.27 m h^{-1} for test W1, 0.88 m h^{-1} for test W2, and 0.022 m h^{-1} for test W3, respectively. The rate of widening for test W2 was 3.3 times greater than that of W1, even

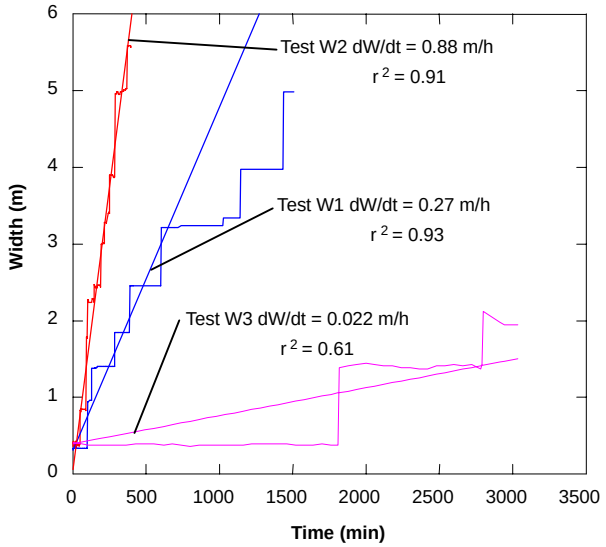

Figure 8. Breach width versus time for tests W1, W2, and W3.

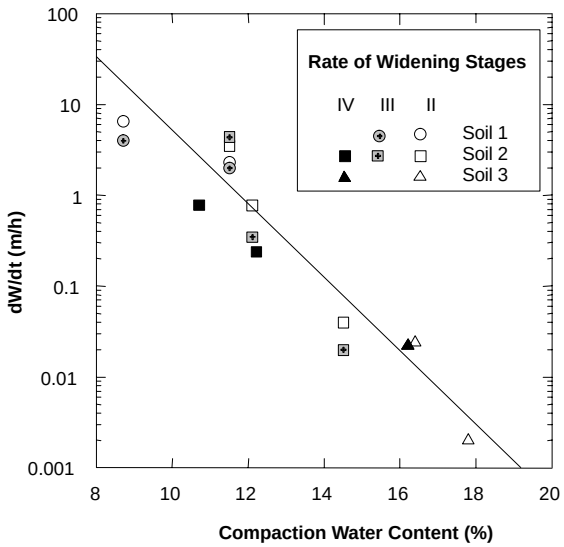

Figure 9. Rate of breach widening (*dW*/*dt*) versus compaction water content.

though the two embankments consisted of the same soil material, and W2 was 40 times greater than W3.

Since the embankment geometry and hydraulic stresses were the same for tests W1 and W2 and the soil materials were the same, the increase in the rate of widening was attributed to differences in material properties due to variations in compaction. The embankments for tests W1 and W2 were constructed with the same homogeneous soil material with the only distinguishable difference being the compaction water content. Hanson et al. (2003a, 2003b) observed that compaction water content had a significant effect on embankment erosion, including both headcut migration and breach widening during stages II and III of embankment erosion. They observed that a 5% point change in water content could result in a 100-fold change in widening rate during stages II and III. The relationship of compaction water content and change in widening rate appeared to be independent of soil type at the same compaction energy and could be expressed as:

$$\Delta \frac{dW}{dt} = 10^{[0.4(\Delta wc\%)]} \quad (1)$$

The change in the average compaction water content from test W1 to test W2 was 1.5% (table 1). Using equation 1, the expected change in widening rate would be 4.0. So the observed variation in widening rate between test W1 and W2 of 3.3 for stage IV is similar to that observed for stages II and III of previous tests. The hydraulic stresses are not the same from stages II and III to that of IV, since stage IV is similar to open channel flow and stages II and III exist as a headcut migration environment. Yet, a comparison of erosion widening rates to the compaction water content for tests W1, W2, and W3 along with the seven previous overtopping tests described by Hanson et al. (2003a) (fig. 9) indicates the importance of compaction water content in influencing the rate of breach widening. It should be noted that all of these embankments, even though constructed of different soil materials, were compacted with the same compaction effort (i.e., the same compaction procedures and equipment) used for tests W1, W2, and W3. This gives the appearance that rate of widening and embankment erosion widening in general are independent of material type and dependent on water content and most likely compaction energy. But in reality material type generally dictates specified compaction water contents during construction in order to attain proper densities and strengths. Therefore, in general, higher clay-type soil materials will have a higher compaction water content specified for construction purposes.

Tinney and Hsu (1961), Visser (1998), and Coleman et al. (1997) concluded that hydraulic stress should play an important part in modeling breach widening as well as other stages of non-cohesive embankment erosion. This would also seem likely for modeling breach widening of cohesive embankments. Therefore, a relationship between the hydraulic stress and rate of breach widening should result in material erodibility values comparable with previously measured values for the soils used in tests W1, W2, and W3. A reasonable starting point in modeling breach widening would be the excess stress equation expressed in terms of the rate of breach widening:

$$\frac{dW}{dt} = 2k_d\left(\tau_{ew} - \tau_c\right) \quad (2)$$

The factor of 2 is included in this equation because erosion on both sides of the notch contributes to the widening rate.

Effective stress on the bed of an open channel is commonly expressed as:

$$\tau_{eb} = \gamma dS \quad (3)$$

The effective stress on the breach sidewall, assuming a rectangular opening, is approximately 0.7 of the stress on the bed (Chow, 1959). As water flows through the breach opening, it passes through critical depth d_c, which can be estimated as 2/3 of the depth of water in the upstream reservoir. Assuming the hydraulic radius is equal to d_c, the energy slope can be determined as a re-arrangement of Manning's equation:

$$S = \left(\frac{gn^2}{d_c^{1/3}}\right) \quad (4)$$

Therefore, the stress on the notch sidewall can be expressed as:

$$\tau_{ew} = 0.7\gamma g\left(d_c^{1/3} n\right)^2 \quad (5)$$

Using equation 5, the stress on the notch sidewall boundary was determined to be 20 Pa, and for purposes of estimating k_d, the critical stress can be assumed to be small (approx. 0). Therefore, k_d can be expressed as:

$$k_d = \left(\frac{\frac{dW}{dt}}{2\tau_{ew}} \right) \quad (6)$$

Based on equation 6, the erodibility coefficients for tests W1, W2, and W3 were determined to be 0.007, 0.022, and 0.0005 m^3 $N\text{-}h^{-1}$, respectively. Hanson et al. (2003a) reported a range of k_d values of 0.007 to 0.029 m^3 $N\text{-}h^{-1}$ for the soil material compacted at similar water contents and efforts as those in tests W1 and W2, and a k_d value of 0.0001 m^3 $N\text{-}h^{-1}$ for soils similar to that used in test W3. This provides two conclusions: (1) the boundary wall stress approach appears a reasonable modeling approach for widening, and (2) the resulting k_d values are comparable with previously measured values.

Summary and Conclusions

Research using large-scale physical models is on-going at the USDA-ARS Hydraulic Engineering Unit to provide a better understanding of how a breach develops over time and what variables influence breach development in cohesive embankments. The erosion and failure process during cohesive embankment overtopping has been described as a four-stage process. Previous studies have not focused on the breach widening process of cohesive embankments during stage IV. The widening process during full breach formation (stage IV) is driven by erosion of the sidewalls and development of an overhang that results in episodic mass failures and widening. Soil properties can greatly influence how a soil erodes; therefore, these properties can affect the rate of breach widening for cohesive embankments. Compaction water content was examined and compared with the breach widening tests presented herein and in previous studies. The comparison indicates a dominance of the soil material compaction properties in influencing the rate of breach widening and that the use of the excess stress equation appears to be a reasonable approach for modeling widening of cohesive embankments. Stress-based algorithms using erodibility parameters were shown to be a reasonable approach to predict the rate of widening during stage IV. These studies provide unique information for describing the breach widening process during stage IV and for future validation and development of computer breach simulation models.

References

Chow, V. T. 1959. *Open-Channel Hydraulics.* New York, N.Y.: McGraw-Hill.

Coleman, S. E., D. P. Andrews, and M. G. Webby. 2002. Overtopping breaching of noncohesive homogeneous embankments. *J. Hydraulic Eng.* 128(9): 829-838.

Coleman, S. E., R. C. Jack, and B. W. Melville. 1997. Overtopping breaching of noncohesive embankment dams. In *Proc. 27th Congress of the IAHR*, D42-D47. Madrid, Spain: International Association for Hydraulic Research.

Hanson, G. J., K. R. Cook, W. Hahn, and S. L. Britton. 2003a. Evaluating erosion widening and headcut migration rates for embankment overtopping tests. ASAE Paper No. 032067. St. Joseph, Mich.: ASAE.

Hanson, G. J., K. R. Cook, W. Hahn, and S. L. Britton. 2003b. Observed erosion processes during embankment overtopping tests. ASAE Paper No. 032066. St. Joseph, Mich.: ASAE.

Pugh, C. A. 1985. Hydraulic model studies of fuse plug embankments. REC-ERC-85-7. Denver, Colo.: U.S. Bureau of Reclamation.

Ralston, D. C. 1987. Mechanics of embankment erosion during overflow. In *Proc. 1987 National Conference on Hydraulic Eng*., 733-738. Reston, Va.: ASCE, Hydraulics Division.

Terzaghi, K. 1941. General wedge theory of earth pressure. In *Proc. ASCE Trans., Part 2* 67(8): 68-97.

Tinney, R. E., and H. Y. Hsu. 1961. Mechanics of washout of an erodible fuse plug, *J. Hydraulics Division of ASCE* 87(3): 1-30.

Visser, P. J. 1998. Breach growth on sand-dikes. In *Communications on Hydraulic and Geotechnical Engineering*. Report No. 98.1. Delft, The Netherlands: Delft University of Technology.

USDA-NRCS. 2005. Watershed rehabilitation: A progress report. Washington D.C.: USDA-NRCS.

Nomenclature

d	= depth of water (m)
d_c	= critical depth (m)
g	= gravitational acceleration (m s^{-2})
k_d	= erodibility coefficient (m^3 $N\text{-}h^{-1}$)
n	= Manning's n
NP	= non-plastic
PI	= plasticity index
Q	= discharge (m^3 s^{-1})
S	= energy grade line slope
WC	= compaction water content (%)
W1, W2, W3	= test identification
dW/dt	= rate of breach widening (m h^{-1})
Δ wc%	= change in compaction water content (%)
Δ dW/dt	= change in widening rate
γ	= specific weight of water (N m^{-3})
γ_d	= dry unit weight of soil (kN m^{-3})
τ_c	= critical stress (Pa)
τ_{eb}	= effective stress on the bed (Pa; 1 Pa = 1 N m^{-2})
τ_{ew}	= effective stress on the breach sidewall (Pa)